ARTICLE
Journal of Cellular Biochemistry 117:66–73 (2016)

Journal of Cellular Biochemistry

In-Silico Template Selection of In-Vitro Evolved Kalata B1 of *Oldenlandia Affinis* for Scaffolding Peptide-Based Drug Design

B. Senthilkumar, Prakash Kumar, and R. Rajasekaran*

Bioinformatics Division, School of Bio Sciences and Technology, Vellore Institute of Technology University, Vellore 632014, Tamil Nadu, India

ABSTRACT

Structural stability of *Oldenlandia affinis* cyclotide, kalata B1 of native (1NB1) and two mutants 2F2I ([P20D, V21K] kB1) and 2F2J ([W19K, P20N, V21K] kB1) was investigated. Single model analysis showed high number of intra-molecular interactions followed by more proportion of beta sheet contents in [P20D, V21K] kB1 as compared to that of native and the other mutant of kalata B1. Further, the modern conformational sampling approach, an alternate to classical molecular dynamics was introduced, which revealed that the [P20D, V21K] kB1 was identified as structurally stable one, substantiated by various structural events viz., root mean square deviation, root mean square fluctuation, and angular deviation by Ramachandran plot. Moreover, the statistically validated contours of polar surface area, hydrogen bond distribution and the distance of disulfide bridges also supported the priority of [P20D, V21K] kB1 with respect to stability. From this work, it is proposed that the [P20D, V21K] kB1 (2F2I) could be the best template for scaffolding peptide based drug design. J. Cell. Biochem. 117: 66–73, 2016. © 2015 Wiley Periodicals, Inc.

KEY WORDS: OLDENLANDIA AFFINIS; CYCLOTIDES; KALATA B1; CONFORMATIONAL SAMPLING; STABILITY

Pharmaceutical companies have recently placed their interest on small molecule drugs, as they are said to be orally available, can be exposed to various body systems and easily taken up by the cells. Peptides are widely accepted for this cause as they are safe, tolerable, efficient, highly selective, potent, and smaller in size [Fosgerau and Hoffmann, 2014; Hennemann et al., 2014]. The usage of cyclic peptides was extended not only in pharmaceutics but also in the field of agriculture as insecticides. One of the major causes for the deteriorating food production in crop plants is insects. The reduction of insect predation is channelized through chemical and biological agents, which contains organic compounds or large biomolecules. As a solution for these complicated methods, cyclotides was substantially preferred as an alternate [Craik, 2012; Fosgerau and Hoffmann, 2014]. Cyclotides are unique family of plant defense proteins possessing an inimitable cyclic backbone and cystine knot [Wang et al., 2011; Gunasekera et al., 2013]. The generic name "cyclotides" (cyclic peptides) has been titled for a rapidly emerging family of macrocyclic polypeptides, which vary around 30 amino acid residues in length and are cyclized with amide bonds of peptide backbone [Craik et al., 1999]. Cyclotides are the largest family of circular proteins, currently comprising more than 160 members, and it is predicted that many thousands await discovery [Simonsen et al., 2005; Wang et al., 2011]. The first cyclotide discovered is kalata B1 (kB1), which was found in an African plant *Oldenlandia affinis* [Gran, 1973], a member of the Rubiaceae plant family. Cyclotide kB1 of *Oldenlandia affinis* is a small plant-derived macrocyclic peptide, a potent insecticide with extreme resistance to proteolysis. The preparation of plant extract by boiling and the oral administration of the same, suggested that kB1 was both thermally stable and bio-available [Gran, 1973]. Their stability is highly commendable among the cyclotides, hence they are highly used in the field of medicine as an excellent template in drug designing [Rosengren, 2003; Colgrave and Craik, 2004]. The peptide kB1 is produced by Oak1 gene, a precursor of 11 kDa which was subsequently shown to comprise 29 amino acids, including six cysteine residues [Craik et al., 1999]. The structure determination revealed the unique features of a head-to-tail cyclized backbone and a core composed of three disulfide bonds (S—S) arranged in a cystine knot motif. In this motif, an embedded ring structure is formed by two S—S bonds and their connecting backbone segment is penetrated by the third S—S bond. The combination of a cystine knot motif embedded within a circular backbone is termed as cyclic cystine knot (CCK) [Craik et al.,

*Correspondence to: Dr. R. Rajasekaran, Associate Professor, School of Bio Sciences and Technology, Bioinformatics Division, Vellore Institute of Technology University, Vellore – 632014, Tamil Nadu, India.
E-mail: rrajasekaran@vit.ac.in

Manuscript Received: 28 January 2015; Manuscript Accepted: 29 May 2015
Accepted manuscript online in Wiley Online Library (wileyonlinelibrary.com): 6 June 2015
DOI 10.1002/jcb.25248 • © 2015 Wiley Periodicals, Inc.

1999, 2001]. The cyclic backbone of kB1 potentially confers advantages over conventional linear proteins, including greater stability and resistance to proteolytic digestion; since circular proteins have no termini, they are resistant to cleavage by exopeptidases. It has been suggested that the rigid nature and stability of *Oldenlandia affinis* kB1 framework makes it useful as a scaffold in drug design [Craik et al., 2001, 2002].

Naturally available peptides fail to be used in convenient therapeutics as they possess low chemical and physical stability. Improving these factors, peptides can offer an enormous growth potential in future therapeutics [Fosgerau and Hoffmann, 2014]. It is noted that, the modified kB1 (variants) played a significant role in the folding and biological activity. It has been used widely as an insecticide and a therapeutic drug in various biological areas like neurotensin binding, uterotonic activity, hemolytic activity, anti-HIV activity, and activity against tumor cells [Gruber et al., 2007]. It also provided an understanding of the tolerance of CCK framework, establishing its viability as a structural scaffold for the development of peptide-based pharmaceuticals [Clark et al., 2006]. From our literature review, a lack of computational studies related to structural stability of native kB1 and its mutants was found. Hence, the structural stability of native kB1 and its mutants was computationally investigated in order to screen the best template for scaffolding future drug design prospects.

MATERIALS AND METHODS

DATASET

Protein Databank [Berman et al., 2000] was used to retrieve the structural coordinates of native and mutants belonging to *Oldenlandia affinis* kB1. The mutant structures was constructed by replacing the hydrophobic patch in loop 5 of 1NB1 (Native) by two and three charged residues in 2F2I ([P20D, V21K] kB1) and 2F2J ([W19K, P20N, V21K] kB1), respectively. The classical force field was used for the structural optimization and refinement, resulting in a well optimized structure as output [Suhre and Sanejouand, 2004]. Hence, the PDB structures of both the native and mutants was subjected to energy minimization using Gromacs force field embedded in NOMAD-Ref program [Suhre and Sanejouand, 2004]. The structurally minimized native and mutants of kB1 was further introduced for single model and ensemble analysis.

COMPUTATION OF INTRA-MOLECULAR INTERACTION AND SECONDARY STRUCTURE DISTRIBUTION

The energy minimized native and mutants of kB1 conformation obtained from the NOMAD-Ref was investigated by the single model based programs viz., Protein interaction calculator (PIC) [Tina et al., 2007] and STRIDE [Heinig and Frishman, 2004]. The study of interactions within and between protein structures highly contributed to the protein stability and function [Nick Pace et al., 2004]. PIC computes the various types of interactions viz., S—S bonds, hydrogen bonds, salt–bridges, hydrophobic residues, aromatic–aromatic, aromatic–sulfur and cation–π interactions in a protein. These interactions was calculated by empirical and semi-empirical set of rules obtained through standard and published data [Tina et al., 2007]. Classification of secondary structure plays a vital role in the identification of stability for the given protein [Trevino et al., 2007]. The STRIDE program was used for computing the secondary structure distribution which was graphically viewed via Polyview-MM [Porollo and Meller, 2010]. STRIDE is a python-scripted program, which utilizes knowledge-based algorithm to give an optimized output after evaluating both the hydrogen bond energy and torsion angles of the residues. The hydrogen bond energy uses empirical energy function calculating the length between donor and acceptor along with their bond angle deviations [Heinig and Frishman, 2004].

CONFORMATIONAL SAMPLING BY NORMAL MODE-BASED GEOMETRIC SIMULATION

The conformational sampling method namely NMSim was used which implements a three-step approach for multi-scale modeling of protein conformational changes. First, the protein structure was coarse-grained using the FIRST software [Jacobs et al., 2001]. Second, a rigid cluster normal-mode analysis provided low-frequency normal modes. Third, this mode was used to extend the recently introduced idea of constrained geometric simulations by biasing backbone motions of the protein, whereas a side chain motion was biased towards favorable rotamer states. The generated structure was iteratively corrected regarding steric clashes and stereochemical constraint violations. The approach allowed performing three simulation types: unbiased exploration of conformational space, pathway generation by a targeted simulation, and radius of gyration-guided simulation. The NMSim approach (conformational sampling) was found to be a computationally efficient alternative to molecular dynamics simulations [Ahmed et al., 2011]. Root Mean Square Deviation (RMSD) and Root Mean Square Fluctuation (RMSF) were generated by the program along with a file containing ensemble models of the given protein. The generated conformations (ensembles) and pathways of conformational transitions could serve as an input for more sophisticated sampling techniques [Ahmed et al., 2011; Kruger et al., 2012].

COMPUTATION OF STRUCTURAL EVENTS FROM ENSEMBLES

The structural and residual variation in the kB1 ensemble structures of native and mutants was calculated using VEGA ZZ and VMD packages. Vega ZZ is a molecular modeling package [Pedretti et al., 2004] used for computing the angular deviation from Ramachandran Plot (RP), Polar Surface Area (PSA), and S—S bond distance for the native and mutant ensembles of kB1 obtained through conformational sampling method. The displacement of the ensemble models and their related residues in accordance to the variation of torsion angles was returned as RMSD, RMSF, and RP [Kempner, 1993; Carlsen et al., 2014; Carrascoza et al., 2014]. The interaction of protein structures with water cavity was calculated as PSA [Vogt et al., 1997], while the compactness earned due to S—S bridges was also computed. The overall distribution of the hydrogen bonds in the given ensemble was calculated using VMD [Humphrey et al., 1996]. VMD is a molecular visualization program used for the display and analysis of large biomolecular structures like proteins and nucleic acids. It

operates on C++ language, an object-oriented design used for the maintenance and addition of latest features. The ensemble protein models obtained through NMSim was analyzed through VMD, thereby calculating the distribution of hydrogen bonds among the models. The obtained result was graphically registered as a chart, depicting the variations in hydrogen bonding capacity of native and mutant types [Humphrey et al., 1996].

STATISTICAL ANALYSIS

The non-parametric value obtained via molecular simulation program was analyzed for statistical significance. Kruskal Wallis test [Kruskal, 1952] an ordinary one-way ANOVA for non-parametric data was performed without assuming Guassian distribution using MS Excel. The non parametric mean values of the native and mutants were compared simultaneously with each other. The significance of each parameter was evaluated by probability value (*P*-value), the *P*-value less than 0.05 was considered statistically significant.

RESULTS

This study was done among the *Oldenlandia affinis* kB1 native, [P20D, V21K] kB1, and [W19K, P20N, V21K] kB1 to identify various parameters that aid in its stability based on two types of analysis. At first, single model analysis through which the various types of intra-molecular interactions and distribution of secondary structures was studied. Second, the dynamic analysis, through which various structural events such as (1) structural deviations, (2) torsion angles, (3) polar surface area, (4) hydrogen bond, and (5) distance of S—S bridge distribution was studied.

STRUCTURAL FEATURE OF KALATA B1 OF NATIVE AND MUTANTS

kB1 is the first cyclotide to be structurally characterized [Rosengren, 2003]. The cartesian coordinate files for the given PDB IDs namely 1NB1, 2F2I, and 2F2J was retrieved from the PDB database. The variation of residues between the native and mutants along with their PDB IDs was given in Table I. It was found that the 2F2I and 2F2J possess two (P20D and V21K) and three (W19K, P20N, and V21K) mutations respectively, compared to that of the native (1NB1) kB1. The presence of S—S bonds provide additional stabilization to a protein structure [Colgrave and Craik, 2004]. In relation to the said statement, the cyclotide also incorporated a cystine knot that embedded a ring in the structure consisting two S—S bonds and a third one that connected the backbone segments [Craik, 2010]. The structural conformer of native kB1 and its mutants along with their mutational positions and S—S bonds was illustrated in Figure 1.

TABLE I. Dataset of Native and Mutants of Kalata B1 With Their Intra-Molecular Interactions (IMIs)

SI no.	PDB ID	Mutation positions	Total no. of IMIs	Reference
1.	1NB1	Native type	75	Rosengren [2003]
2.	2F2I	P20D/V21K	83	Clark et al. [2006]
3.	2F2J	W19K/P20N/V21K	66	Clark et al. [2006]

Further refinement of energy minimization was carried out for both the native type and mutants of kB1 using GROMACS force field for conformational sampling analysis.

SINGLE MODEL ANALYSIS OF INTRA-MOLECULAR INTERACTIONS AND SECONDARY STRUCTURE

The energy-minimized structures of kB1 was subjected into single model analysis. The intra-molecular interaction (IMIs) was calculated using the program PIC. The calculated values displayed a various number of IMIs that has taken place in the given protein, kB1 of *Oldenlandia affinis*. The results obtained from PIC showed a large number of IMIs in [P20D, V21K] kB1 (83) than that of the native (75) and [W19K, P20N, V21K] kB1 (66), as shown in Table I.

While checking the distribution of secondary structures using STRIDE, an increase in the number of beta sheets among the mutants ([P20D, V21K] kB1 and [W19K, P20N, V21K] kB1) compared to that of the native type was observed. The obtained result was charted using Polyview-MM, the program displayed the varying residues and its position constituting for secondary structures (Fig. 1).

STRUCTURAL DEVIATIONS RENDERING STABILITY

The RMSD and RMSF were calculated from the trajectory data generated through NMSim. The structural variations are said to play a major role in the stability of protein [Unsworth et al., 2007]. While viewing the graphical representation of both RMSD and RMSF in Figure 2A, the mean RMSD structural deviations was found to be less between the native (1.93 Å) and its mutants ([P20D, V21K] kB1–1.90 Å and [W19K, P20N, V21K] kB1–2.12 Å) with a significant statistical (*P*-value <0.0001) value. These values suggested the presence of deviations among the native and mutant structures. On the other hand, RMSF (Fig. 2B) values of the mutants ([P20D, V21K] kB1–0.94 Å and [W19K, P20N, V21K] kB1–1.06 Å) residues showed a marked increase in rigidity compared to that of native (1.15 Å) (*P*-value <0.0001).

The changes in ψ and ϕ angles abrupt polypeptide conformation, thus proper distribution of torsion angles among the residues of a protein determines the level of stability in a protein [Korn and Rose, 1994]. The angular deviation in the ensemble of kB1 native and mutants was calculated using Ramachandran plot in Vega ZZ trajectory analysis. Ramachandran map presents the basic understanding of the stereochemistry of polypeptide backbone. For ages, it has been used routinely for the validation of protein structures identified through various experimental methods or modified via computational tools [Lakshmi et al., 2014]. The overall mean value of the exactness of Ramachandran plot showed varied percentage among native (75.75%) and mutants ([P20D, V21K] kB1–77.56% and [W19K, P20N, V21K] kB1–75.16%) as diagrammatically portrayed in Figure 2C. The results showed [P20D, V21K] kB1 with greater percentage of Ramachandran plot exactness, thus indicating the change in angular deviations (*P*-value <0.0001) caused due to mutation as a reason behind the improved stereochemical stability [Dahl et al., 2008]. Polar surface area (PSA) is defined as a sum of surfaces of polar atoms (usually oxygens, nitrogens, and attached hydrogens) in a given molecule. The polar atoms (O, S, N, P, and H not bonded to C) and apolar atoms (C and H bonded to C) was calculated based on their atom surface existence. As noted

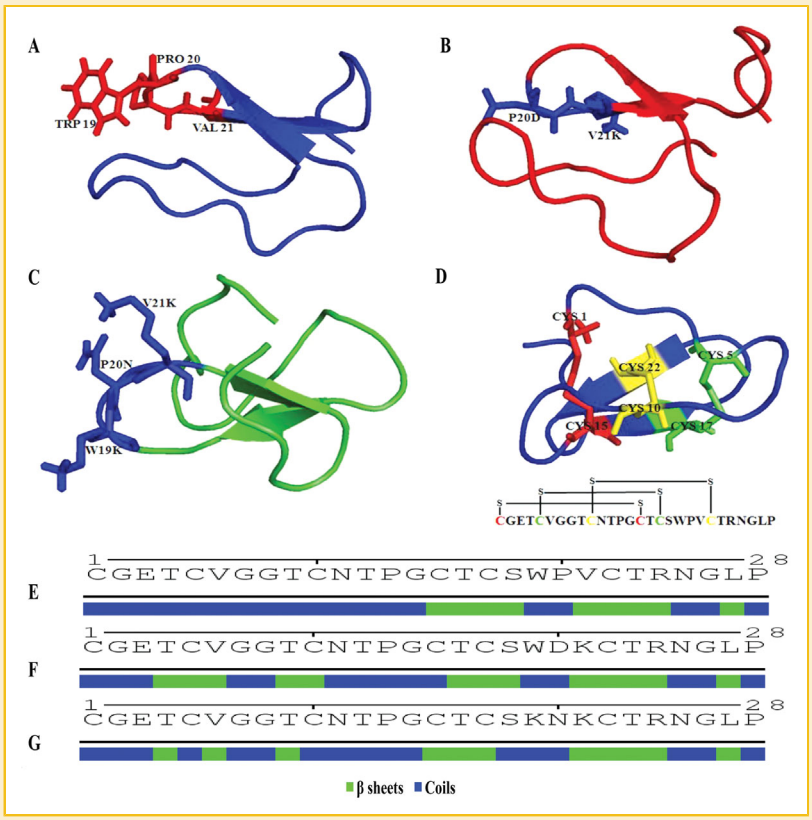

Fig. 1. Ribbon diagram of the enzyme kalata B1 (*Oldenlandia affinis*) with mutations as stick model. (A) Native (blue) with positions involved in mutations (red); (B) [P20D, V21K] kB1 (red) with mutation sites (blue); (C) [W19K, P20N, V21K] kB1 (green) with mutation sites (blue); (D) positional illustration of native disulfide bridges along with their secondary structure distribution in (E) native, (F) [P20D, V21K] kB1 and (G) [W19K, P20N, V21K] kB1.

previously, the PSA increased consequently along with hydrogen bonding density to water which in turn increases thermostability [Vogt et al., 1997]. Recent studies have explained the correlation of PSA and membrane permeability which is a boon to peptide drug designing [Stenberg et al., 1999]. The PSA mean data showed an increase in mutants ([P20D, V21K] kB1–1137.168 $Å^2$ and [W19K, P20N, V21K] kB1–1155.698 $Å^2$) when compared with the native (1090.742 $Å^2$) using Vega ZZ [Gaillard et al., 1994] which is represented in Figure 2D with statistical significance (*P*-value <0.0001). Further, the presence and distribution of hydrogen bonds in the ensembles of native and mutants was identified to understand the stability in depth.

DISTRIBUTION OF HYDROGEN BONDS IN KALATA B1 ENSEMBLES OF NATIVE AND MUTANTS

Hydrogen bonds are electrostatic interactions with strong affinity at non-polar environments. Various studies showed that hydrogen bonds contribute favorably to protein stability and packing density [Vogt et al., 1997; Nick Pace et al., 2014]. As a consequence, the distribution of hydrogen bonds was calculated in the ensemble of proteins with the parameters set at a distance of 3.5 Å and the angle between the acceptor and donor was set at 30° [Durrant and McCammon, 2011]. In that case, the number of hydrogen bonds was counted for every ensemble models of native and mutants and their mean values was calculated as a parametrical term, which is graphically represented in Figure 3. The calculated mean was further analyzed to find their percentage differences between the native and mutant ensembles. Accordingly, the percentage difference between the kB1 native and mutant [P20D, V21K] kB1 was found to be 66% whereas the other mutant [W19K, P20N, V21K] kB1 showed 62% only.

DEVIATION OF DISTANCE AMONG S—S BRIDGES IN KALATA B1 CONFORMERS OF NATIVE AND MUTANTS

Kalata B1 contains six conserved cysteine residues giving rise to three S—S bridges. The cyclic backbone and S—S topology together form a cyclic cystine knot, which is referred significantly as the reason for increased stability of kB1 [Daly et al., 2009; Wang et al., 2009]. Thus, imparting the essentiality of computational analysis for the study of S—S bond distance and their distribution among the ensemble models of both kB1 native and mutants. The positional tier of S—S bridges forming cyclic cystine knot was located between C1-C15, C5-C17, and C10-C22 residues [Rosengren, 2003]. The differences in bond distance among the three S—S bridges of kB1 ensembles was observed using Vega ZZ package. The statistically differentiated (*P*-value <0.0001) bond distance of S—S bridges in both native and [W19K, P20N, V21K]

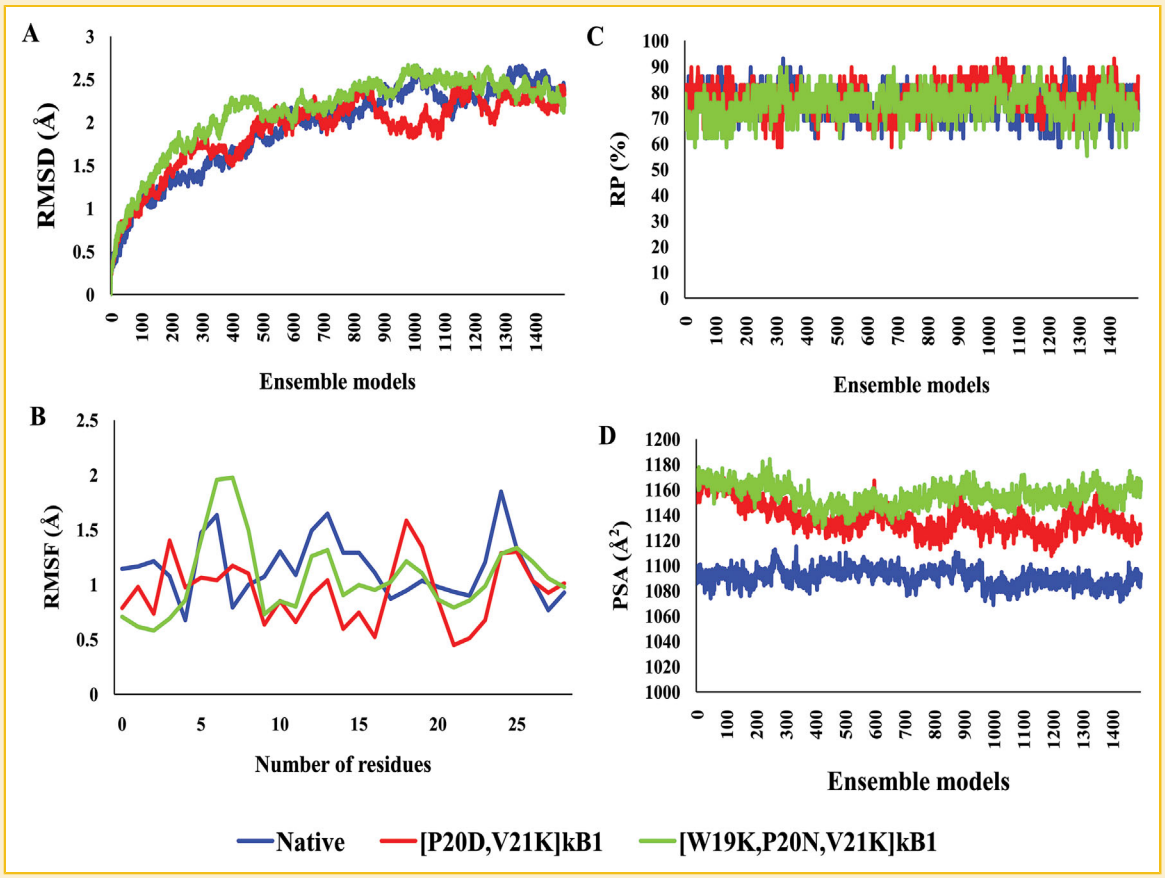

Fig. 2. Structural events of native kalata B1 and its mutants; (A) Root Mean Square Deviation (RMSD); (B) Root Mean Square Fluctuation (RMSF); (C) Ramachandran Plot (RP); and (D) Polar Surface Area (PSA).

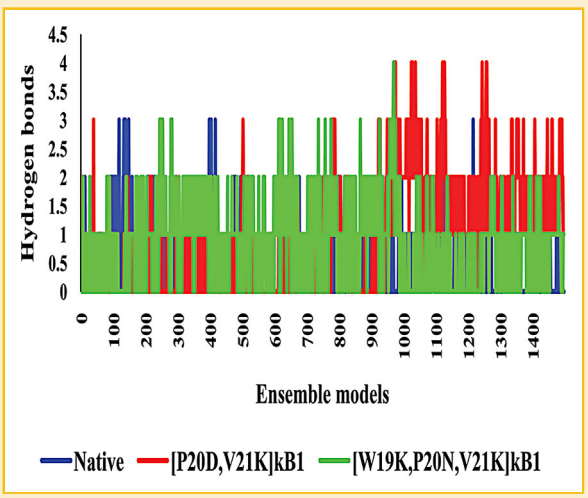

Fig. 3. Distribution of Hydrogen bonds in the ensemble of native and mutants [P20D, V21K] kB1 and [W19K, P20N, V21K] kB1 of kalata B1.

kB1 ensembles was distributed widely between the range of 2.01 Å and 2.04 Å. On the other hand, the ensembles of [P20D, V21K] kB1 displayed a closer arrangement of S—S bridges ranging between 2.01 Å and 2.03 Å, as shown in Figure 4 with statistical significant *P*-value less than 0.0001. The former thus reduced the compactness whereas the latter increased the structural compactness by reducing the overall structure of kB1.

The mean bond distance of S—S bridges among the ensembles of native and mutants gave a wider and general idea about the kB1 compactness. In addition, studies involving the variability in S—S bond distance and its distribution from ensembles within a defined range in the form of cluster enlightened us more on the effect of S—S bridges in regard to kB1 stability (Table II and Fig. 4). Thus, the clustered bond length data of the S—S bridges was calculated between distances ranging 2.01 Å–2.02 Å, 2.02 Å–2.03 Å, 2.03 Å–2.04 Å, and 2.04 Å–2.05 Å. As a result, the clustered data forming S—S bridge of C1-C15 was found to show 79.44% in native at a distance ranging 2.01 Å–2.02 Å, while it was found to be 94.5% and 76.4% at a distance ranging 2.02 Å–2.03 Å in [P20D, V21K] kB1 and [W19K, P20N, V21K] kB1, respectively. Similarly, that of C5-C17 was found to be 93.2% in native at a distance ranging 2.03 Å–2.04 Å, while it was found to be 75.5% and 60.1% at a distance ranging 2.02 Å–2.03 Å in [P20D, V21K] kB1 and [W19K, P20N, V21K] kB1,

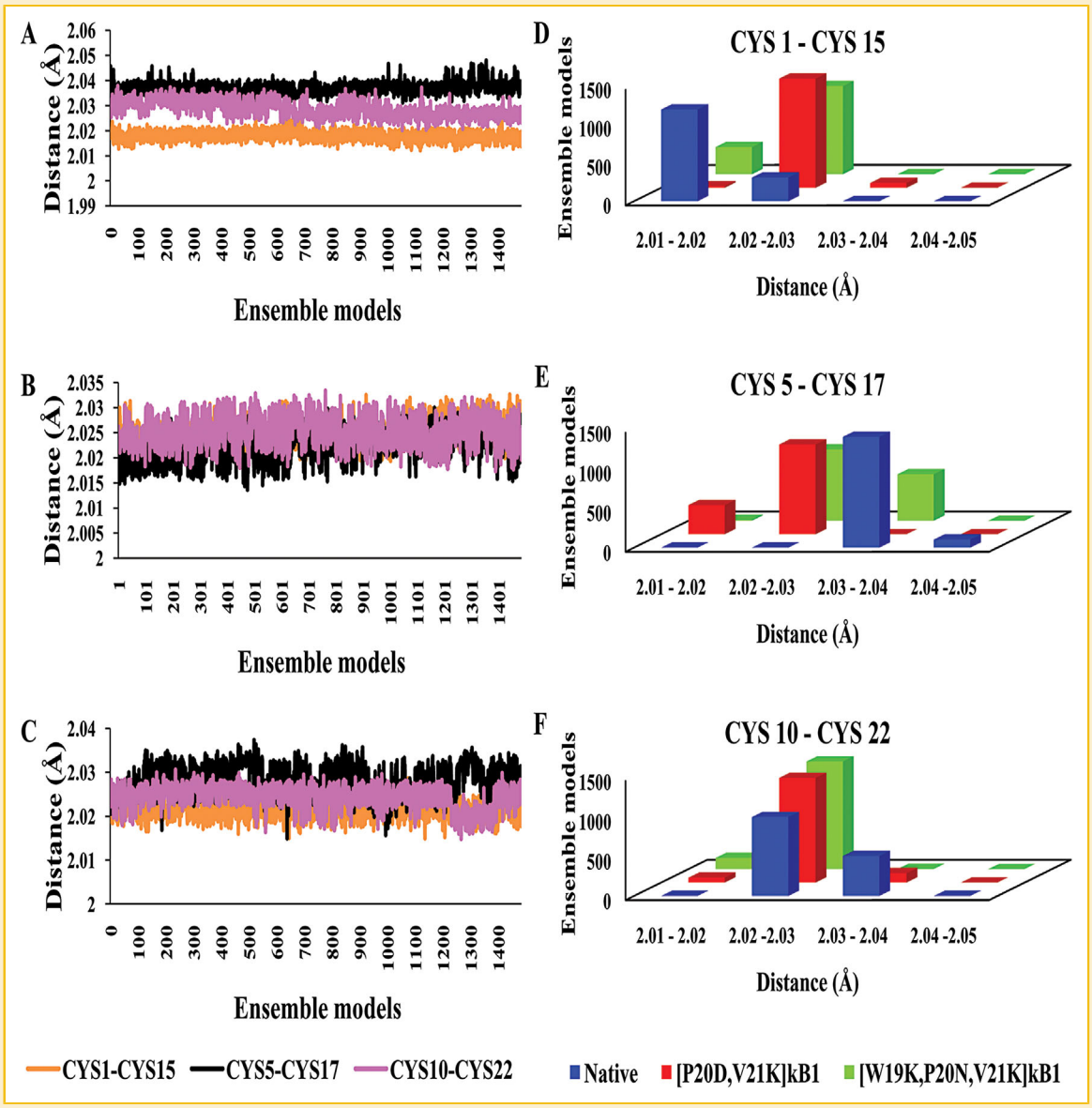

Fig. 4. S—S bond distance in the ensemble models of (A) native; (B) [P20D, V21K] kB1; and (C) [W19K, P20N, V21K] kB1 mutants of kalata B1. The clustered models differentiating the positional distribution of conformers between native kalata B1 and its mutants, pertaining to their S—S bond distance; (D) CYS 1–CYS 15; (E) CYS 5–CYS 17; and (F) CYS 10–CYS 22.

respectively. Further, the clustered data forming S—S bridge of C10-C22 at a distance ranging 2.02 Å–2.03 Å was found to be 66.4%, 88.1%, and 90.5% in native, [P20D, V21K] kB1 and [W19K, P20N, V21K] kB1, respectively. However, at a distance ranging 2.01 Å–2.02 Å, it was found to be 4.1% and 9.4% only in [P20D, V21K] kB1 and [W19K, P20N, V21K] kB1, respectively.

In native, C1-C15 was found to exist at a closer distance ranging 2.01 Å–2.02 Å for larger percentage of ensemble models, while the other S—S bridges (C5-C17 and C10-C22) was found to exist distantly. On the other hand, the three S—S bridges viz., C1-C15, C5-C17, and C10-C22 was found to exist at a distance ranging 2.02 Å–2.03 Å for larger percentage of both ([P20D, V21K] kB1 and [W19K, P20N, V21K] kB1) the ensemble models of mutants. In particular, the [P20D, V21K] kB1 was found to show much larger percentage of ensemble models at a distance ranging 2.02 Å–2.03 Å with all the three S—S bridges. It is to be noted that, though the native showed larger percentage of ensemble models with C1-C15 at a distance ranging 2.01 Å–2.02 Å, it failed to establish the same with the other two S—S bridges (C5-C17 and C10-C22).

DISCUSSION

The kB1 of *Oldenlandia affinis* has been a well-known plant derived cyclotide, a family of proteins with cyclic backbone and cystine knot widely used in the field of agriculture, medicine, and pharmacy. High

TABLE II. Clustered Data of S—S Bridges and Their Variation at Different Positional Tier Pertaining to the Bond Distance Among the Native and Mutants of kB1 Along With Their *P*-Values

			Range of bond distance (Å)				
SI no.	PDB IDs	Positional tier of S—S bridges	2.01–2.02	2.02–2.03	2.03–2.04	2.04–2.05	Kruskal Wallis test (*P*-value)
1	1NB1 Ensembles	C1-C15	1190	308	0	0	<0.0001
		C5-C17	0	0	1396	102	
		C10-C22	0	995	503	0	
2	2F2I Ensembles	C1-C15	20	1416	62	0	<0.0001
		C5-C17	367	1131	0	0	
		C10-C22	61	1319	118	0	
3	2F2J Ensembles	C1-C15	354	1144	0	0	<0.0001
		C5-C17	12	900	586	0	
		C10-C22	141	1356	1	0	

resistance to heat, chemicals, and enzymatic degradation was noted in the cyclotides with cyclic cystine knot hence it has been largely preferred in pharmaceutical industry. The values pertaining to intramolecular interactions calculated using the program PIC, displayed a various number of interactions between the native and mutants of *Oldenlandia affinis* kB1. The results affirmed a change in molecular level assist in the stability of [P20D, V21K] kB1 significantly. In addition, the distribution of secondary structures using STRIDE conveyed an increase in beta sheets in [P20D, V21K] kB1 comparatively. Thus, obtained results proposed the significant change in characteristics of kB1 might be due to mutations, thus suggesting further parametrical understanding by ensemble analysis.

Conformational sampling was used to analyze various structural events with the ensemble of proteins obtained; RMSD results lacked great differences, but the RMSF exhibited a significant rigidity in [P20D, V21K] kB1 compared to native and [W19K, P20N, V21K] kB1. Thus, these results suggested that a slight deviation in the structure could induce major changes in the protein. In addition, the torsion angles calculated using the Ramachandran plot verified the relativity in organization and distribution of secondary structures thereby increasing [P20D, V21K] kB1 rigidity. The polar surface area and the presence of hydrogen bonds also favored the [P20D, V21K] kB1. On the whole, these parameters showed [P20D, V21K] kB1 to be highly stable than the native and other mutant which was experimentally proved by Clark, Daly, and Craik [Clark et al., 2006].

Cyclic cystine knot, a well-studied factor ideal for the protein stability and compactness of cyclotide kB1 was studied in regard to its distance and distribution via cluster analysis. The six cysteine molecules of kB1 was connected via S—S bonds whose distance was expressed graphically based on proximal arrangement among native and two mutants ensemble. The differences in short interatomic distances calculated from MD simulated structures (about 0.01Å) play a critical role in the analysis of structure-based simulations, enzymatic reactions, and drug designing [Kuzmanic et al., 2011]. Hence, the arrangement of S—S bonds in native and [W19K, P20N, V21K] kB1 varied in distances ranging between 2.01 Å and 2.04 Å with a decrease in compactness. Whereas in [P20D, V21K] kB1, the S—S bonds was arranged closely ranging between 2.02 Å and 2.03 Å contributing to the increased compactness of [P20D, V21K] kB1 corresponding to its increased stability. However, the overall results conveyed that [P20D, V21K] kB1 possessed significant S—S bond distance than the native and the other mutant. Thereby contributing to its increased compactness and stability which has been stated experimentally earlier by Clark et al [Clark et al., 2006], which opened the possibility in pharmaceutical usage.

In conclusion, the effect of various physiochemical parameters that aided for the stability of kB1 mutants was observed computationally. The need for a stable peptide in the field of drug designing had been a vital factor for ages, where the improvement of cyclotides like kB1 could be a boon for the pharmaceutical industry. The study concluded by selecting [P20D, V21K] kB1 (2F2I) as a starting point for designing a stable peptide-based drug.

ACKNOWLEDGMENT

The authors thank the management of Vellore Institute of Technology University for providing the facilities and encouragement to carry out this research work.

REFERENCES

Ahmed A, Rippmann F, Barnickel G, Gohlke H. 2011. A normal mode-based geometric simulation approach for exploring biologically relevant conformational transitions in proteins. J Chem Inf Model 51:1604–1622.

Berman HM, Westbrook J, Feng Z, Gilliland G, Bhat TN, Weissig H, Shindyalov IN, Bourne PE. 2000. The protein data bank. Nucleic Acids Res 28:235–242.

Carlsen M, Koehl P, Rùgen P. 2014. On the importance of the distance measures used to train and test knowledge-based potentials for proteins. PloS ONE 9:e109335.

Carrascoza F, Zaric S, Silaghi-Dumitrescu R. 2014. Computational study of protein secondary structure elements: Ramachandran plots revisited. J Mol Graph Model 50:125–133.

Clark RJ, Daly NL, Craik DJ. 2006. Structural plasticity of the cyclic-cystine-knot framework: Implications for biological activity and drug design. Biochem J 394:85–93.

Colgrave ML, Craik DJ. 2004. Thermal, chemical, and enzymatic stability of the cyclotide kalata B1: The importance of the cyclic cystine knot. Biochemistry (Mosc) 43:5965–5975.

Craik DJ, Daly NL, Bond T, Waine C. 1999. Plant cyclotides: A unique family of cyclic and knotted proteins that defines the cyclic cystine knot structural motif. J Mol Biol 294:1327–1336.

Craik DJ, Daly NL, Waine C. 2001. The cystine knot motif in toxins and implications for drug design. Toxicon Off J Int Soc Toxinol 39:43–60.

Craik DJ, Simonsen S, Daly NL. 2002. The cyclotides: Novel macrocyclic peptides as scaffolds in drug design. Curr Opin Drug Discov Devel 5:251–260.

Craik DJ. 2010. Discovery and applications of the plant cyclotides. Toxicon 56:1092–1102.

Craik DJ. 2012. Host-defense activities of cyclotides. Toxins 4:139–156.

Dahl DB, Bohannan Z, Mo Q, Vannucci M, Tsai J. 2008. Assessing side-chain perturbations of the protein backbone: A knowledge-based classification of residue Ramachandran space. J Mol Biol 378:749–758.

Daly NL, Rosengren KJ, Craik DJ. 2009. Discovery, structure and biological activities of cyclotides? Adv Drug Deliv Rev 61:918–930.

Durrant JD, McCammon JA. 2011. HBonanza: A computer algorithm for molecular-dynamics-trajectory hydrogen-bond analysis. J Mol Graph Model 31:5–9.

Fosgerau K, Hoffmann T. 2014. Peptide therapeutics: Current status and future directions. Drug Discov Today DOI: 10.1016/j.drudis.2014.10.003

Gaillard P, Carrupt PA, Testa B, Boudon A. 1994. Molecular lipophilicity potential, a tool in 3D QSAR: Method and applications. J Comput Aided Mol Des 8:83–96.

Gran L. 1973. On the effect of a polypeptide isolated from "Kalata-Kalata" (Oldenlandia affinis DC) on the oestrogen dominated uterus. Acta Pharmacol Toxicol (Copenh) 33:400–408.

Gruber CW, Cemazar M, Anderson MA, Craik DJ. 2007. Insecticidal plant cyclotides and related cystine knot toxins. Toxicon Off J Int Soc Toxinol 49:561–575.

Gunasekera S, Aboye TL, Madian WA, El-Seedi HR, Göransson U. 2013. Making ends meet: Microwave-accelerated synthesis of cyclic and disulfide rich proteins via in situ thioesterification and native chemical ligation. Int J Pept Res Ther 19:43–54.

Heinig M, Frishman D. 2004. STRIDE: A web server for secondary structure assignment from known atomic coordinates of proteins. Nucleic Acids Res 32:W500–W502.

Hennemann H, Wirths S, Carl C. 2014. Cell-based peptide screening to access the undruggable target space. Eur J Med Chem DOI: 10.1016/j.ejmech.2014.10.038

Humphrey W, Dalke A, Schulten K. 1996. VMD: Visual molecular dynamics. J Mol Graph 14:33–38,27–28.

Jacobs DJ, Rader AJ, Kuhn LA, Thorpe MF. 2001. Protein flexibility predictions using graph theory. Proteins 44:150–165.

Kempner ES. 1993. Movable lobes and flexible loops in proteins. Structural deformations that control biochemical activity. FEBS Lett 326:4–10.

Korn AP, Rose DR. 1994. Torsion angle differences as a means of pinpointing local polypeptide chain trajectory changes for identical proteins in different conformational states. Protein Eng 7:961–967.

Kruger DM, Ahmed A, Gohlke H. 2012. NMSim Web Server: Integrated approach for normal mode-based geometric simulations of biologically relevant conformational transitions in proteins. Nucleic Acids Res 40:W310–W316.

Kruskal WH. 1952. A nonparametric test for the several sample problem. Ann Math Stat 23:525–540.

Kuzmanic A, Kruschel D, van Gunsteren WF, Pannu NS, Zagrovic B. 2011. Dynamics may significantly influence the estimation of interatomic distances in biomolecular X-ray structures. J Mol Biol 411:286–297.

Lakshmi B, Ramakrishnan C, Archunan G, Sowdhamini R, Srinivasan N. 2014. Investigations of Ramachandran disallowed conformations in protein domain families. Int J Biol Macromol 63:119–125.

Nick Pace C, Scholtz JM, Grimsley GR. 2014. Forces stabilizing proteins. FEBS Lett 588:2177–2184.

Nick Pace C, Trevino S, Prabhakaran E, Martin Scholtz J. 2004. Protein structure, stability and solubility in water and other solvents. Philos Trans R Soc B Biol Sci 359:1225–1235.

Pedretti A, Villa L, Vistoli G. 2004. VEGA-an open platform to develop chemo-bio-informatics applications, using plug-in architecture and script programming. J Comput Aided Mol Des 18:167–173.

Porollo A, Meller J. 2010. POLYVIEW-MM: Web-based platform for animation and analysis of molecular simulations. Nucleic Acids Res 38: W662–W666.

Rosengren KJ. 2003. Twists, knots, and rings in proteins. STRUCTURAL DEFINITION OF THE CYCLOTIDE FRAMEWORK. J Biol Chem 278:8606–8616.

Simonsen SM, Sando L, Ireland DC, Colgrave ML, Bharathi R, Göransson U, Craik DJ. 2005. A continent of plant defense peptide diversity: Cyclotides in Australian Hybanthus (Violaceae). Plant Cell 17:3176–3189.

Stenberg P, Luthman K, Artursson P. 1999. Prediction of membrane permeability to peptides from calculated dynamic molecular surface properties. Pharm Res 16:205–212.

Suhre K, Sanejouand Y-H. 2004. ElNemo: A normal mode web server for protein movement analysis and the generation of templates for molecular replacement. Nucleic Acids Res 32:W610–W614.

Tina KG, Bhadra R, Srinivasan N. 2007. PIC: Protein interactions calculator. Nucleic Acids Res 35:W473–W476.

Trevino SR, Schaefer S, Scholtz JM, Pace CN. 2007. Increasing protein conformational stability by optimizing β-Turn sequence. J Mol Biol 373:211–218.

Unsworth LD, van der Oost J, Koutsopoulos S. 2007. Hyperthermophilic enzymes—stability, activity and implementation strategies for high temperature applications: Properties and applications of hyperthermozymes. FEBS J 274:4044–4056.

Vogt G, Argos P. 1997. Protein thermal stability: Hydrogen bonds or internal packing? Fold Des 2:S40.

Vogt G, Woell S, Argos P. 1997. Protein thermal stability, hydrogen bonds, and ion pairs. J Mol Biol 269:631–643.

Wang CK, Hu SH, Martin JL, Sjögren T, Hajdu J, Bohlin L, Claeson P, Göransson U, Rosengren KJ, Tang J, Tan NH, Craik DJ. 2009. Combined X-ray and NMR analysis of the stability of the cyclotide cystine knot fold that underpins its insecticidal activity and potential use as a drug scaffold. J Biol Chem 284:10672–10683.

Wang CKL, Clark RJ, Harvey PJ, Johan Rosengren K, Cemazar M, Craik DJ. 2011. The role of conserved glu residue on cyclotide stability and activity: A structural and functional study of kalata B12, a naturally occurring glu to asp mutant. Biochemistry (Mosc) 50:4077–4086.